Proceedings of PSFVIP-5
5th Pacific Symposium on Flow Visualisation and Image Processing
27-29th September 2005, Australia

PSFVIP-5-251

FULL-SCALE HIGH-SPEED "EDGERTON" RETROREFLECTIVE SHADOWGRAPHY OF EXPLOSIONS AND GUNSHOTS

G.S. Settles[1], T.P. Grumstrup[1], J.D. Miller[1], M.J. Hargather[1], L.J. Dodson[1], J.A. Gatto[2]
1. Gas Dynamics Lab, Mechanical and Nuclear Engineering Department, Penn State University, University Park PA 16802 USA
2. Transportation Security Lab, US Transportation Security Administration, W. J. Hughes Technical Center, Atlantic City, NJ 08405 USA
Corresponding author: G.S. Settles, Fax (814) 865-0118, Email: gss2@psu.edu

Abstract: Almost ½ century ago, H. E. "Doc" Edgerton demonstrated a simple and elegant direct-shadowgraph technique for imaging large-scale events like explosions and gunshots. Only a retroreflective screen, flashlamp illumination, and an ordinary view camera were required. Retro-reflective screens have been used for shadowgraphy in the interim, but the unique combination of large-scale, simplicity and portability offered by this approach has barely been tapped. In particular, Edgerton's retroreflective shadowgraph is available for use in applications hostile to most optical diagnostics, such as full-scale outdoor daylight field testing of explosives and weapons, and homeland security research. Also in the interim different retroreflective materials have appeared, though 3M's Scotchlite™ brand is still among the best. In particular, though, digital high-speed cameras are rapidly replacing the older film-camera technology. Here we have used a 2.4 m square retroreflective screen and continuous point-source illumination from a powerful xenon arc lamp. The lamp casts a shadowgram on the screen that is recorded at 1 μs frame exposure and at various frame rates and resolutions using a Photron APX CMOS digital camera. Examples are shown of an explosion and the discharge of several different firearms. The ability to quickly and easily acquire high-speed digital shadowgraph movies in hostile environments is especially helpful in visualizing the time-dependent physics of such complicated events as those examined here.

1 Introduction

Recent papers [1-2] by the present authors discuss efforts to provide optical instrumentation for homeland security research involving explosions and related phenomena of high-speed physics. Shadowgraph and schlieren methods [3] have served similar purposes for over a century, but the traditional field-of-view of these instruments is too small for full-scale shock wave studies. Achieving a significantly-larger field-of-view requires a different approach, such as the large lens-and-grid schlieren instrument described in [2,3]. Here, however, a simpler approach is taken using shadowgraphy.

1.1 Historical review

Shadowgraphy as a flow visualization method was invented by Robert Hooke around 1672, using only the sun and a white surface upon which to cast the shadow [3]. Centuries went by, though, before it was first applied to ballistics. Today the "direct" shadowgraph technique differs from that of Hooke mainly in the use of improved light sources and screens upon which to cast the shadow. While Toepler, Mach, and Boys used open electric sparks to illuminate high-speed physics, Harold E. "Doc" Edgerton (1903-1990) of MIT originated the electronic flashlamp, or strobe [4], and is justifiably famous for it. Almost ½ century ago Edgerton demonstrated a simple and elegant direct-shadowgraph technique

for imaging large-scale events like explosions and gunshots [5]. Only a retroreflective screen, strobe illumination, and an ordinary view camera were required. To demonstrate its robustness, Edgerton photographed the shadowgram of a detonator explosion outdoors in daylight (see Fig. 6.14a of [3]).

The intervening years saw many applications of shadowgraphy but few of Edgerton's retroreflective-screen technique. It did see some use in ballistics research, for example at the German-French Institut Saint-Louis (ISL) and at the historic Krupp Firing Range in Germany [6]. Here a beamsplitter was first used to avoid the double-imaging of solid objects inherent in Edgerton's approach, described below.

The technique was reinvented by Parthasarathy et al. [7] – who did not cite Edgerton's precedent – as a method of visualizing helicopter rotor tip vortices. They called it "wide-field shadowgraphy," but this is something of a misnomer, for shadowgrams had been cast of wide fields before using traditional illumination methods. Nonetheless the rotor studies are a proper use of Edgerton shadowgraphy; they invoke its simplicity, high gain, high speed, and robustness in the face of a potentially-dangerous test subject. A number of subsequent rotor tip vortex investigations by various investigators followed suit, e.g. [8, 9].

1.2 Goals

A search of Science Citation Index reveals that we are the only authors citing Edgerton's original retroreflective shadowgraph paper [5]. Thus, to acknowledge Edgerton's role and for simplicity, we here refer to the combination of direct shadowgraphy, a retroreflective screen, and high-speed imaging as "*Edgerton shadowgraphy*." The present goals are to describe some recent improvements in the method (especially the use of a modern high-speed video camera), and to demonstrate Edgerton shadowgraphy's simplicity and versatility for high-speed imaging of shock wave-generating events.
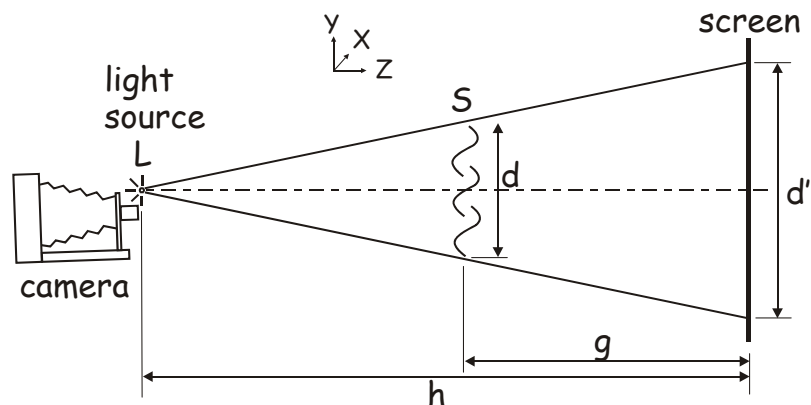

Figure 1. Diagram of Edgerton's direct shadowgraph technique.

2 Experimental Methods
2.1 Principles of direct shadowgraphy

Direct shadowgraphy with diverging illumination is almost too simple to have any principles, but see Ch. 6 of [3] for a discussion of sensitivity and resolution. Briefly, as sketched in Fig. 1, a transparent object S of height d is located at distance g from a screen. Illuminated by a "point" source of light L at distance h from the screen, S projects a spot of height d'. Refractive disturbances in S bend light rays from their original paths, casting a shadow pattern on the screen. According to [3] the sensitivity of this *shadowgram* is near its maximum when S is located within the range $0.3 < g/h < 0.7$. Since S is thus roughly

halfway between the light source and screen, the diameter d of the field-of-view can be roughly half that of the screen, d′. The purpose of the camera in Fig. 1 is to photograph the shadowgram that forms on the screen. If the camera is slightly offset from the light source as described by Edgerton [4,5] and shown here, then solid objects in S will be slightly double-imaged in the resulting shadowgram. Overall, only a screen, light-source, and camera are required for Edgerton's version of direct shadowgraphy. The screen is physically separate of necessity, but the camera and light source may be conveniently combined into a single assembly.
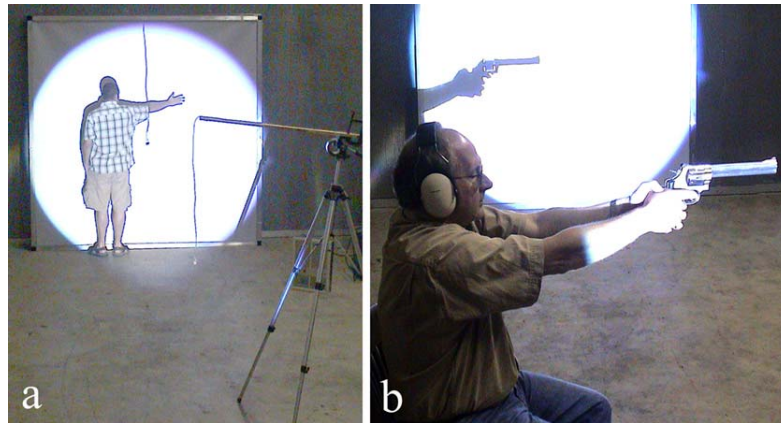

Figure 2. a) An explosive charge is suspended by a wire in the foreground while M. J. Hargather stands before the retroreflective screen in the background. b) J. D. Miller prepares to fire a Smith & Wesson .44 Magnum revolver, positioned in the field-of-view by observing its shadow on the screen.

2.2 Retroreflective screen

Retroreflective screen material returns orders of magnitude greater illumination to the camera than the simple diffuse white screen used for shadowgraphy since antiquity [3]. For high-speed shadowgraphy, a retroreflective screen is a necessity. Ideally it functions like a spherical reflector, returning much of the incident light to its point of origin. The retroreflective screen material used here is 3M Scotchlite™ 7610, a high-gain, industrial-grade, exposed-lens, diffuse gray retroreflective plastic-based sheet material [10]. Only 0.1 mm thick, its back side is pre-coated with a pressure-sensitive adhesive and covered with a removable protective liner. It comes in rolls 0.6 m wide by 46 m long. The manufacturer claims a 900x luminance factor compared with a plain white screen. This and other details of Scotchlite™ 7610 performance vs. that of other retroreflective materials were examined by Winburn et al. [11]. At least one commercial firm [12] manufactures durable screens by mounting Scotchlite™ 7610 to a supporting substrate. The present 2.4 m square screen and backing was made this way, and cost about $4000US. It is stretched across a simple square aluminum frame for stability, Fig. 2.

2.3 Camera/illuminator assembly

A continuous light source of high luminous exitance and small dimensions is needed for high-speed shadowgraph illumination and videography. We use a 1000 W ozone-free xenon arc lamp (Newport/Oriel Instruments). The arc-lamp housing contains the bulb, collimating lens, cooling apparatus, and arc ignition circuitry. The power supply requires a standard 120 VAC electrical source and can be remotely operated. This equipment is sensitive to high temperature and humidity when used outside the laboratory, and requires active external cooling in order to function properly under such conditions.

The heart of the present shadowgraph apparatus is a Photron Ultima APX-RS digital video camera [13]. Its CMOS image sensor provides 1024x1024 (i.e. 1 Mb) frame resolution at frame rates up to 3000 fr/s. Alternatively it can record at 10,000 fr/s with 512x512 pixel resolution, and is capable of 250,000 fr/s at reduced image size. Frame exposure is independently controllable down to 1 μs. A fiber-optic link connects the APX-RS to its controlling laptop computer, upon which the results are viewed (Fig. 3a). The camera acquires 18 Gb of image data in 6 real-time seconds of memory. Rapid events require no triggering, since the camera records continuously and overwrites its memory until stopped. Results are immediately available for viewing and download. Remote camera operation is also provided by the fiber optic link. The camera is rated for a 100g shock, and has survived while imaging powerful explosions as described later.

Figure 3. a) Real-time shadowgram image on laptop computer controlling the APX-RS digital video camera. b) APX camera and zoom lens with clear filter and rod mirror installed.

A flaw in Edgerton's original method [4,5] is the slightly-off-axis location of the camera with respect to the light-source axis (Fig. 1). This can be improved in various ways [14], such as by the use of a beamsplitter [6], though at the cost of ¾ of the beam intensity. Here, however, the arc lamp output is focused to about a 3 mm circle on the camera axis, where a small 45° mirror is installed. Using RTV™ silicone rubber, a 10 mm diameter "rod mirror [15]" is attached to the center of a clear filter that fits over the camera lens, which is a Nikon f/2.8 35-70 mm zoom lens in the present case (Fig. 3b). This provides perfectly-coincident shadowgram illumination with no double-imaging, as well as excellent gain in the collection of retroreflected light by the camera lens. No loss of shadowgram quality is noticed due to the small amount of lens occlusion by the rod mirror.
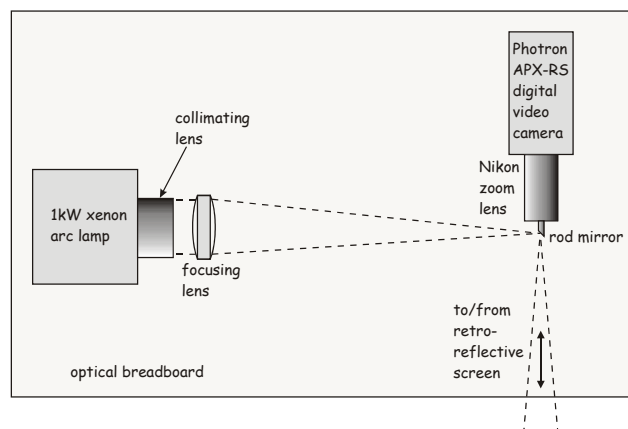

Figure 4. Schematic top view of camera/illuminator assembly mounted to an optical breadboard.
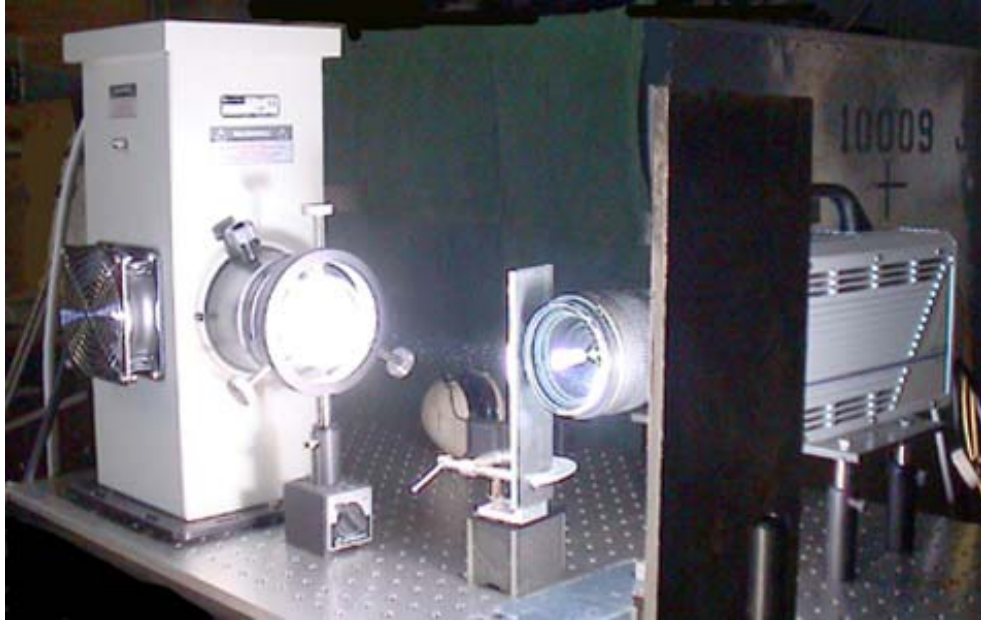
Figure 5. Oblique side view of camera/illuminator assembly (vertical plates are beam stops).

3 Results and Discussion

The results presented in the following two subsections were all taken during the morning of May 26, 2005. The present space allocation does not allow all results from these tests to be shown. Therefore only a selection of high-resolution 1024x1024-pixel shadowgrams taken at 3000 fr/s and 1 μs exposure per frame is shown in order to highlight the near-photographic resolution of the shadowgraph system and digital video camera. Unless otherwise noted, each figure shows a set of frames beginning before the event initiation and stepping 333 μs between frames. Admittedly, time resolution is sacrificed for image resolution at this frame rate and some phenomena require faster framing. Here, however, the field-of-view is large and, with a dozen or more frames spanning each event, interesting physics is clearly revealed.

3.1 Explosion shadowgrams

Fig. 6 shows a small "point" explosion produced by the detonation of 1 gram of triacetone triperoxide (TATP) in a cardboard cylinder initiated by a glow-plug (see also Fig. 2a). The set of APX-camera frames in Fig. 6 shows 9 consecutive stages of this explosion over a total interval of 2.7 ms. Debris from the explosion is hurled at supersonic speeds, and both the primary and secondary spherical blast waves are revealed. Shadowgraph videography of such explosions can be used to determine the TNT equivalent of various explosive mixtures by tracking shock Mach number vs. time using methods described in [16].

There is a future opportunity here for cheap, safe, quick simulations of blast effects using scale models and shadowgraphy. Such scaled experiments compare well with costly, dangerous, time-consuming tests using large explosive charges, e.g. [17]. Scale model explosions can simulate shock diffraction and overpressures about planned buildings, blast mitigation, interior blasts and aircraft hardening, blast containment, and materials fragmentation under shock loading.
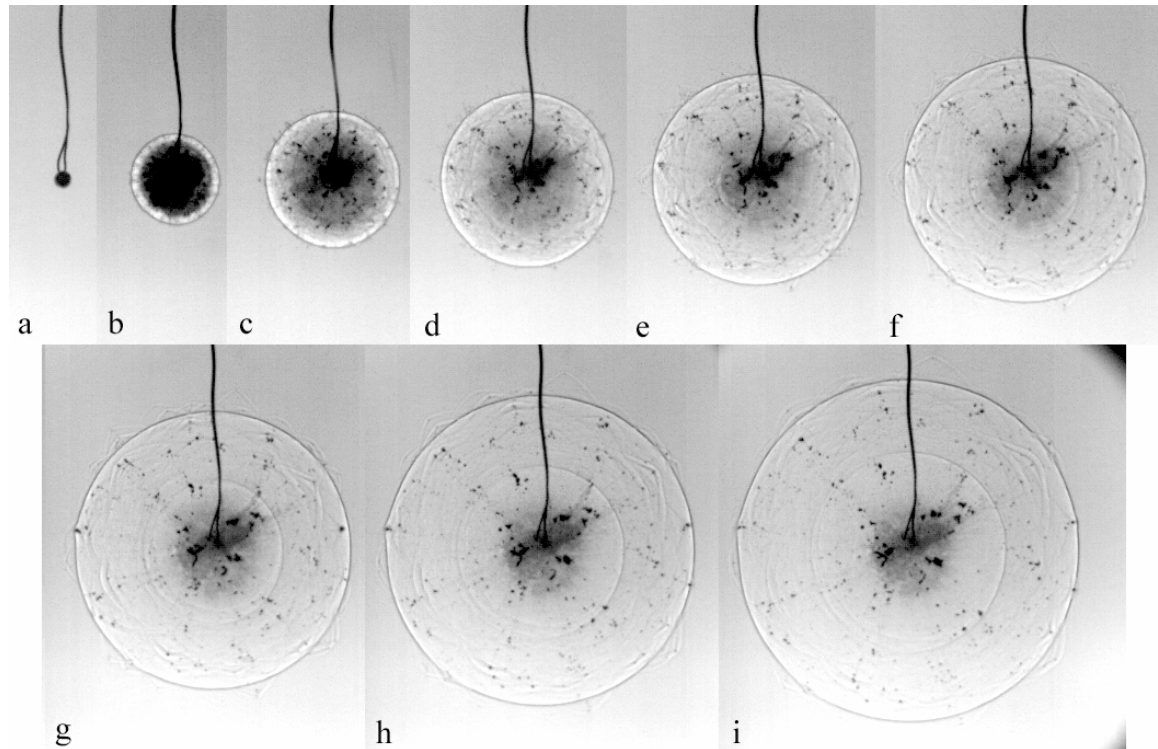
Figure 6. Shadowgram sequence showing the explosion of 1 gram of triacetone triperoxide (TATP) in a cardboard cylinder. Each succeeding frame is exposed for 1 μs and follows its predecessor by 333 μs.

Figure 7. Three of the firearms tested here: a) Smith & Wesson .500 Magnum revolver, b) Heckler & Koch USP Tactical pistol, .45ACP, firing American Eagle ammunition, shown with B&T ImpulsII-A suppressor, c) AK-47 submachine gun with 30 cm barrel, firing 7.62x39 ammunition.

3.2 Gunshot shadowgrams

Eight different weapons were tested, of which 3 are shown in Fig. 7. Resulting sequences of high-speed gunshot shadowgrams are shown in Figs. 8-13. These were taken with a massive bullet stop, permission from the PSU campus police, and all appropriate safety precautions. Previous optical images of gunshots [2,3] were usually limited by the physical dimensions of the optics and could thus visualize only part of the firearm discharge phenomena. Here the shadowgram field-of-view is roughly a 1.3 m circle, often revealing much of the entire process. This makes Edgerton shadowgraphy readily

applicable to many areas of firearms research, such as forensic investigation of point-blank gunshot wounds, shooter hearing protection, shock wave propagation and reflection, and military firearms development. Shadowgrams like these of a shooter, a weapon, and a target could provide valuable information on how the external ballistics develops over time and how that might affect a crime scene.
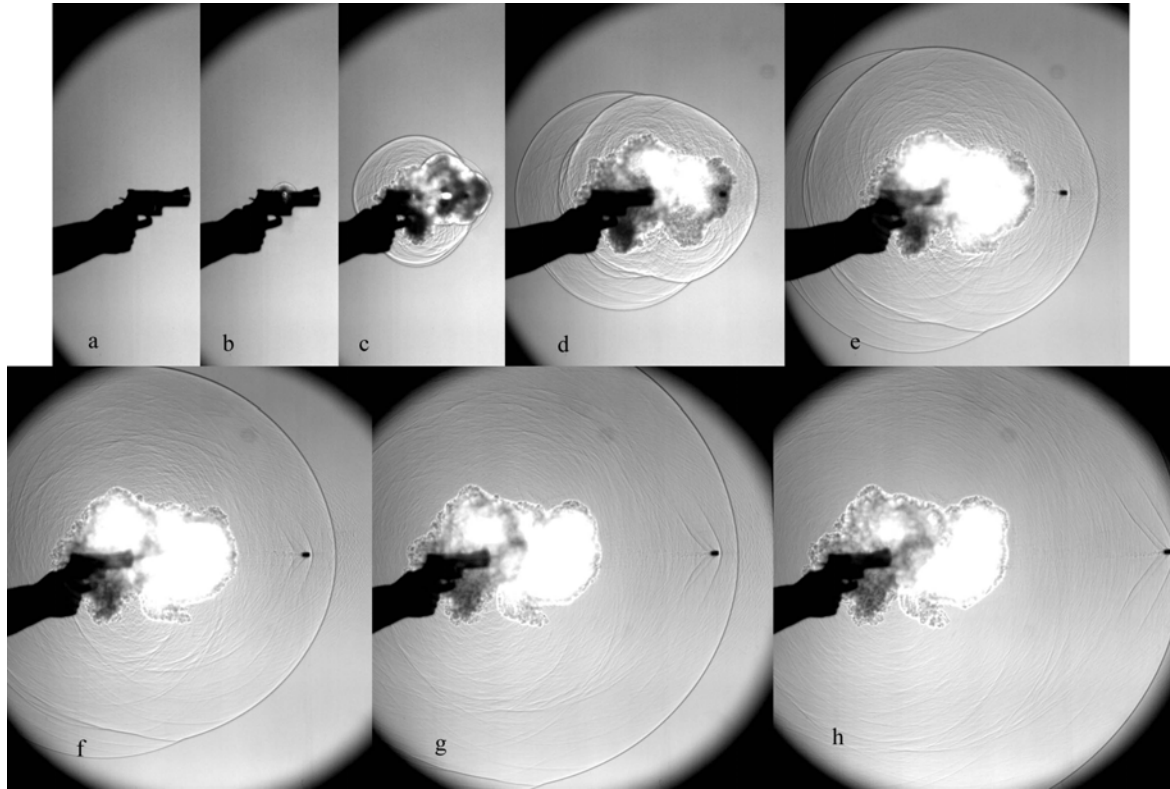

Figure 8. Eight consecutive shadowgrams of the firing of a Smith & Wesson .500 Magnum revolver.

3.2.1 Smith & Wesson .500 Magnum revolver As shown in Fig. 8, this massive handgun ejects clouds of combustion products from both its cylinder and muzzle, driving separate blast waves that appear most clearly in frames d and e. Waves about the bullet show that it is slightly supersonic. The luminosity of the combustion products, despite the 1 µs frame exposure, is quite remarkable. This shadowgram series vividly illustrates how the shooter acquires gunpowder residue on his hands.

3.2.2 Heckler & Koch USP tactical pistol, .45ACP Fig. 9 shows four selected frames from firing this pistol with and without a CCF Swiss B&T ImpulsII-A suppressor. Without the suppressor, powder gases expand laterally after the bullet, driving a strong muzzle-blast wave that causes a loud report. We can compare this with the explosion of Fig. 6, where liberated gas expands spherically, driving a spherical shock wave. The purpose of a suppressor is to reduce the strength of this muzzle blast, and thus the audible report. Figs. 9c and d show that this succeeds in that the lateral gas expansion is suppressed and two separate, visibly-weaker muzzle blast waves result. Also note the generation of jet noise in frame 9d as combustion gases exit forward, following the bullet, in the form of a supersonic jet. Jet noise is perceived as a hiss or screech, not as a report. Peak measurements with a CEL-328 Sound Level Meter, taken along with the shadowgrams, indicated about a 17 dB sound reduction due to the suppressor. Freemesser

[18] describes the function of a suppressor as slowing and cooling the propellant gases. Preventing lateral expansion is also important, based on present results. With shadowgraphy and the application of gas dynamic principles, further advances in suppressor design are possible.
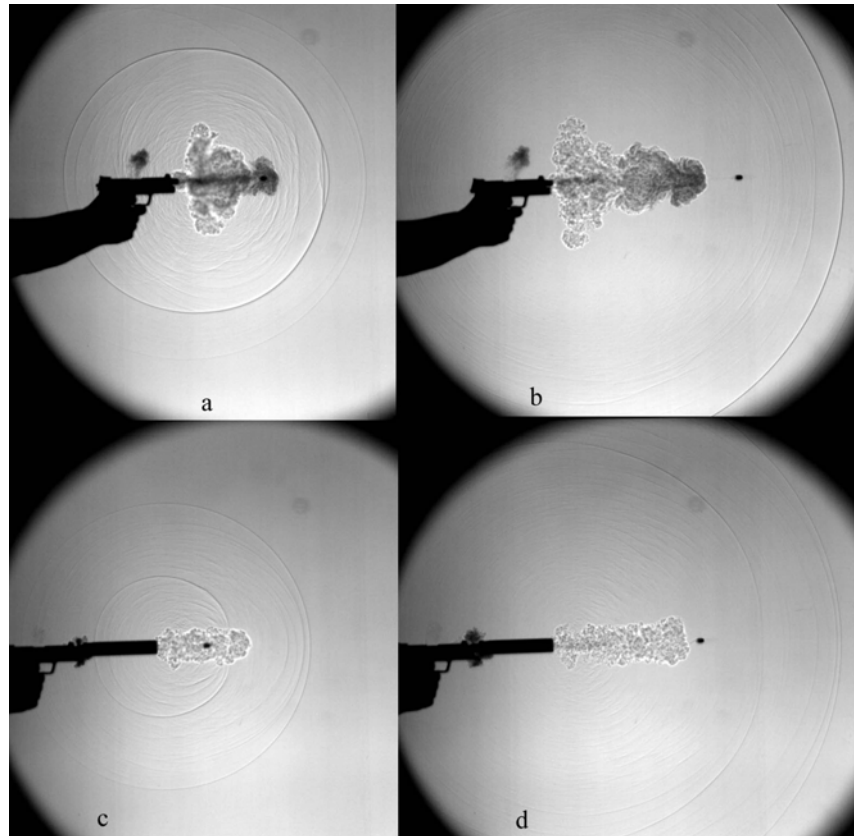

Figure 9. Shadowgrams of the firing of a Heckler & Koch USP Tactical pistol, .45ACP. Without ImpulsII-A suppressor: a) 1.33 ms after firing, and b) 2.33 ms after firing. With suppressor: c) 1.33 ms after firing, and d) 2.33 ms after firing.
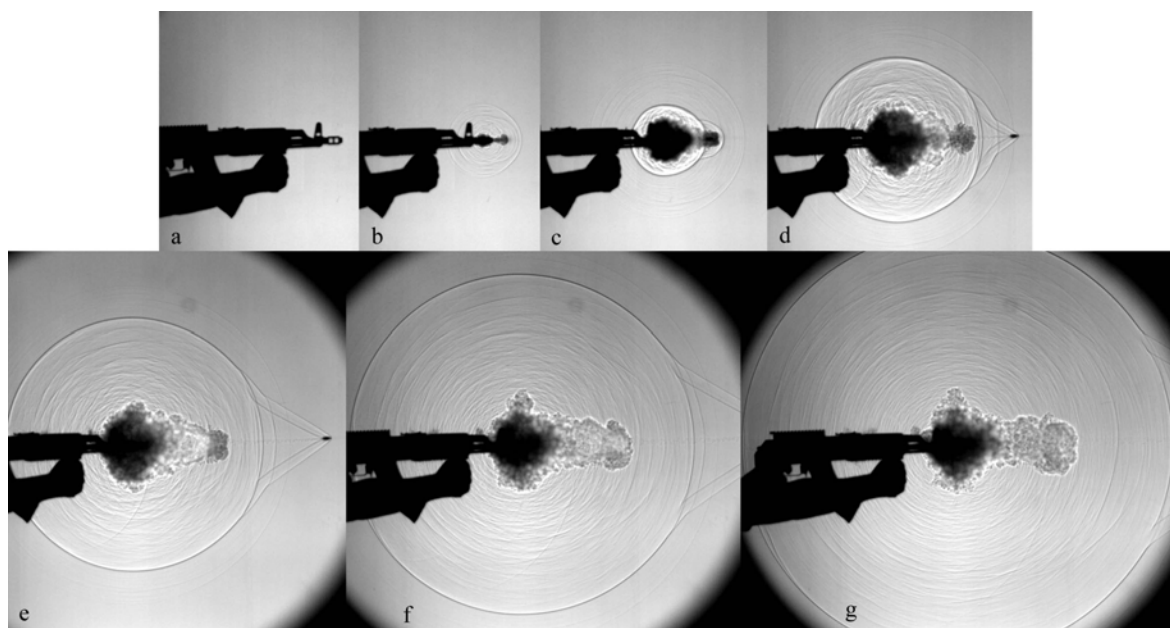

Figure 10. Seven consecutive shadowgrams of the firing of an AK-47 submachine gun (single shot mode). The frame rate is 3000 fr/s and the individual frame exposure time is 1 µs.

3.2.3 AK-47 This legendary and ubiquitous submachine gun, with a 30-cm barrel and firing 7.62x39 ammunition, produces a loud spherical muzzle blast and propels a supersonic bullet as shown in Fig. 10. The interaction between the bullet shocks and the muzzle blast in Figs. 10d and e are quite striking.
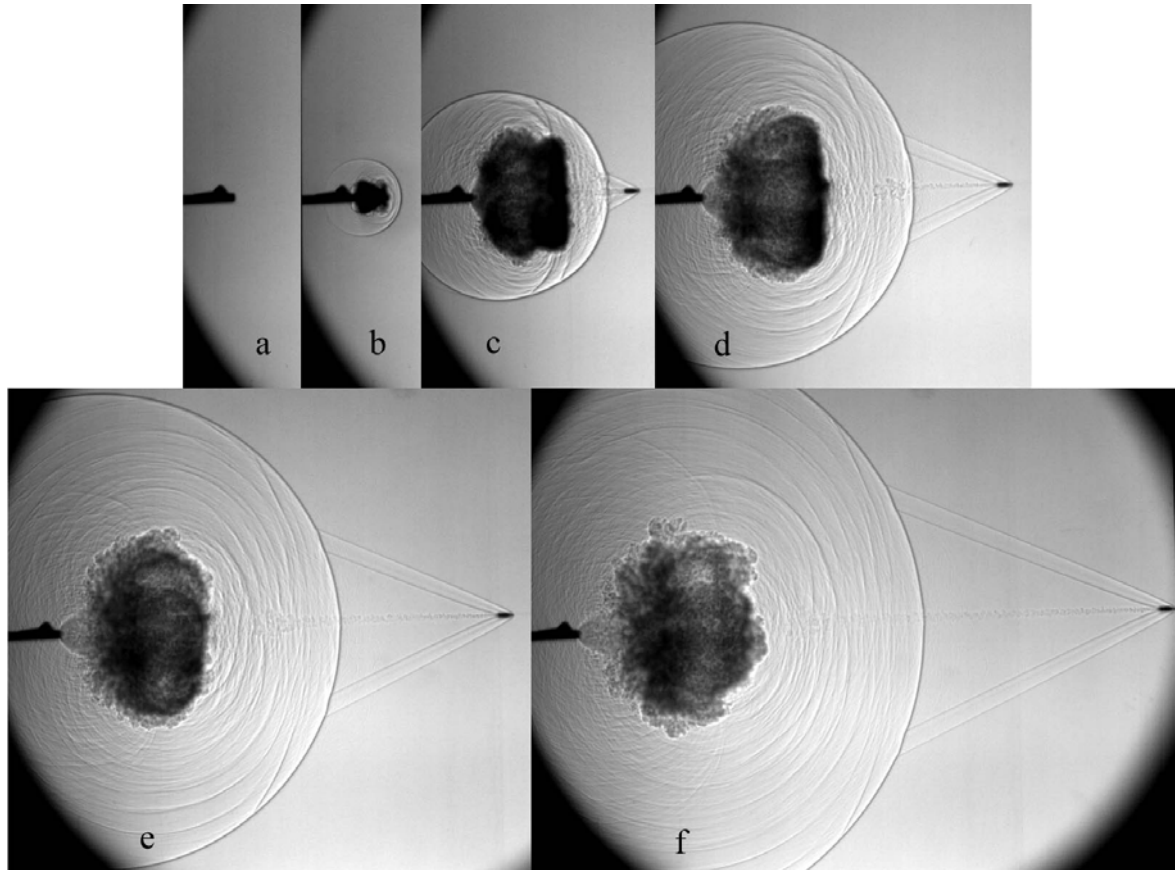

Figure 11. Six consecutive shadowgrams of the firing of a Remington .30-06 deer rifle.

3.2.4 Remington .30-06 high-powered rifle Fig. 11 shows the highly-underexpanded supersonic jet of powder gases exiting the rifle muzzle and forming a toroidal vortex. These expanding gases drive a strong muzzle blast wave, from which the bullet emerges at a Mach number of about 2.5. Similar images were published by Schardin in 1942 [19], but with a much-smaller field-of-view.

3.2.5 Smith & Wesson .44 Magnum revolver   As shown in Fig. 12, this revolver generates less propellant gas and optical disruption than the .500 Magnum discussed earlier. The muzzle blast is preceded by a strong gas emission from the cylinder, and two separate blast waves are clearly seen in frames 12d-f. As before, the shooter's hand is enveloped in a cloud of powder gas. The bullet is observed to be transonic.

3.2.6 Pennsylvania State Police Beretta .40 caliber Model 96D pistol In contrast to most of the weapons examined above, here we observe the firing of the standard handgun issued to Pennsylvania State Troopers: the .40 Caliber Beretta, firing Winchester Ranger 180 grain SXT ammunition (Fig. 13). Propellant gas following the bullet generates a second muzzle blast wave following the first. The absence of waves attached to the bullet shows that it travels at subsonic speed.
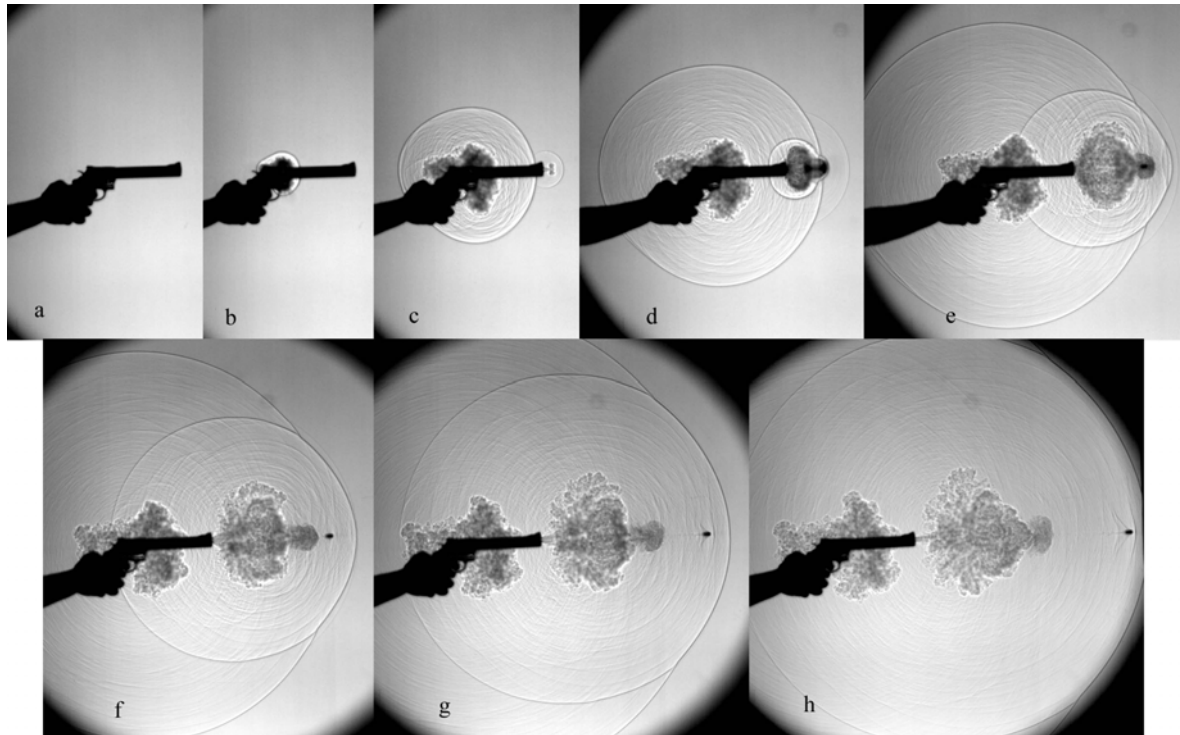
Figure 12. Eight consecutive shadowgrams of the firing of a Smith & Wesson .44 Magnum revolver.
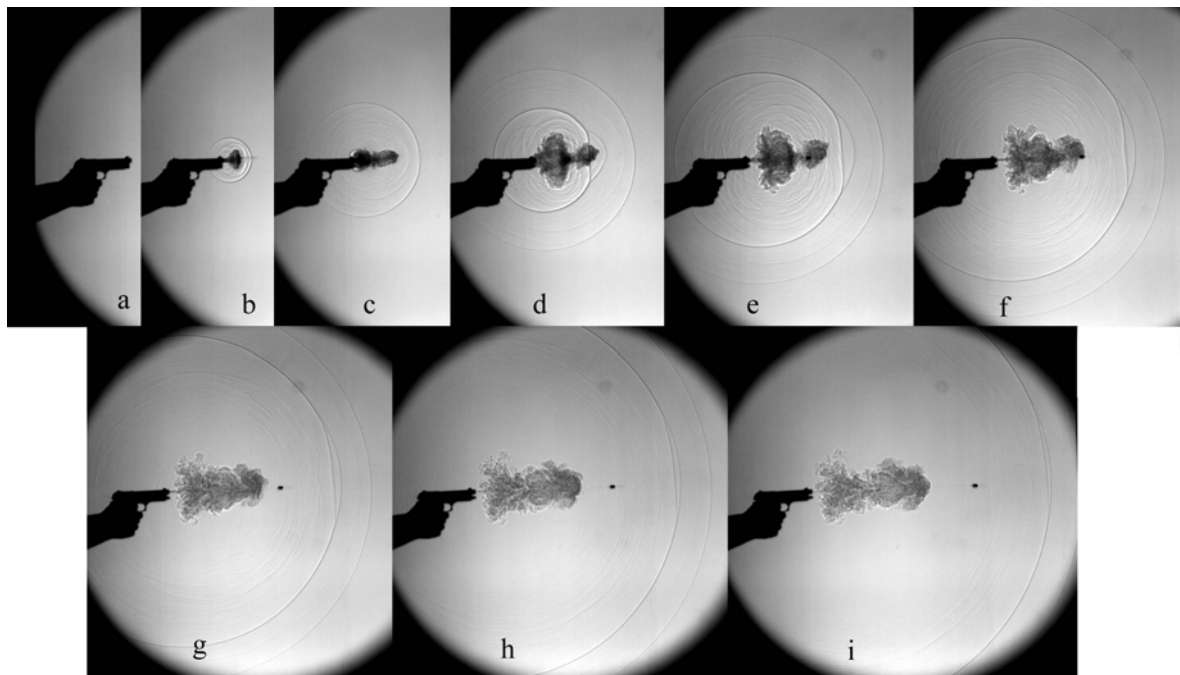

Figure 13. Nine consecutive shadowgrams of the firing of a Pennsylvania State Police Beretta Model 96D.

3.3 Field tests

A unique feature of the Edgerton shadowgraph system is its ability to "go on the road." Its simplicity and robust components make it easy to transport and set up in the outdoors and at remote locations. There are, however, some important considerations in planning such an excursion. In June 2005 the present setup was used in full-scale homeland-security-related explosion experiments at the Fire Safety Test Enclosure of the US Army's Aberdeen Test Center in Maryland. The retroreflective screen was almost 5 m square, or

four times as large as the screen used in our previous experiments reported above. An armored enclosure protected the camera/illuminator assembly from damage due to powerful blast waves and high-speed fragments. Air conditioning was required in this enclosure to prevent heat buildup, especially in the case of the Newport/Oriel Arc Lamp. A port in the side of the armored enclosure provided an optical path for shadowgraphy. The port faced away from the explosion and featured a sacrificial mirror to protect the internal optics from fragment impact. During these tests the experimenters were located in a separate building some 20 meters distant. Thus, remote operation of the video camera was necessary. The APX-RS camera is easily controlled from a distance using the Photron software and fiber-optic link described earlier.

Of many experiments conducted during this 4-day field excursion, two examples are shown here. Fig. 14a shows the explosion of an RP-83 exploding-bridge-wire detonator [20]. The detonator contains slightly over a gram of high explosive (PETN and RDX) in a metal cylinder of 7 mm diameter by 40 mm length. The vertical scale of Fig. 14a is about 1.2 m. The detonator hurls shrapnel laterally ahead of its spheroidal blast wave, but also fires the end of its metal cylinder upward at a spectacular speed (reckoned from the shock angle to be about Mach 7).
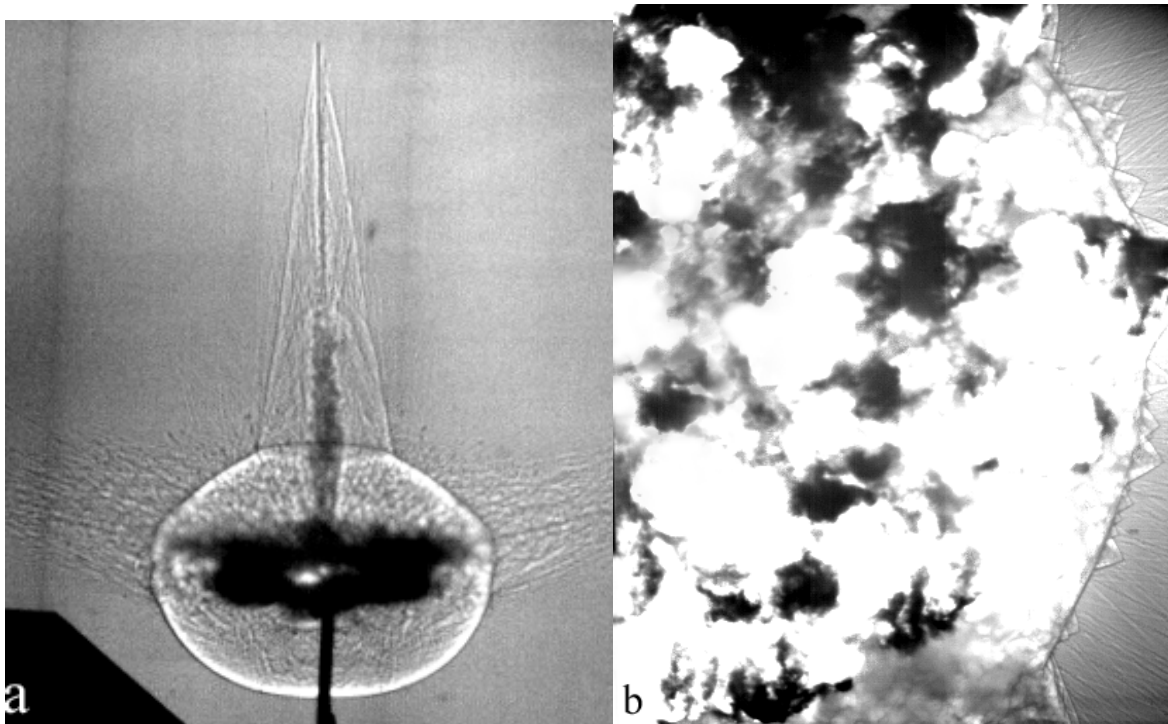

Fig. 14 – a) RP-83 detonator some 400 μs after detonation. b) 0.45 kg C-4 charge about one millisecond after detonation. The frame exposure is 1 μs in both cases.

Fig. 14b is a shadowgram of the explosion of a 0.45 kg ball of bare C-4 plastic explosive (RDX in a putty-like matrix). The fireball radius of about 1.2 m is also the lateral width of the field-of-view in this shadowgram, and the explosion center is near the middle of the left side. The spherical blast wave is seen emerging from the fireball at the right, punctuated by supersonic fragments. Shadowgraphy during the first millisecond of this explosion was obscured by the brilliant direct light of the early fireball.

4 Conclusions

We have shown that Edgerton's 1958 retroreflective shadowgraph method holds new promise in the 21st century, given a few improvements that especially include a modern digital video camera. The method is simple to apply and the quality of the results is impressive enough that this approach ought to see broad use in the investigation of all sorts of full-scale and scale-model explosive and ballistic events, even outdoors and in hostile environments. Even though this approach is less sophisticated than our Full-Scale Schlieren System [2,3], the resulting shadowgrams reveal shock waves and turbulence very effectively. Future improvements should include brighter shadowgram illumination, e.g. by use of a flashlamp or a pulsed laser/bandpass filter combination, in order to minimize fogging due to direct light from explosive events.

5 Acknowledgements

6 References

1. G. S. Settles, B. T. Keane, B. W. Anderson, and J. A. Gatto. Shock waves in aviation security and safety. *Shock Waves,* Vol. 12(4), pp. 267-275, 2003.

2. G. S. Settles, T. P. Grumstrup, L. J. Dodson, J. D. Miller, and J. A. Gatto. Full-scale high-speed schlieren imaging of explosions and gunshots. Proc. 26th Intl. Conf. on High-Speed Photography and Photonics, Alexandria, VA. D. L. Paisley, ed., SPIE Volume 5580, pp. 60-68, 2004.

3. G. S. Settles. Schlieren and shadowgraph techniques: Visualizing phenomena in transparent media. Springer-Verlag, Berlin, 2001.

4. H. E. Edgerton. Electronic flash, strobe. MIT Press, Cambridge, MA, 1970.

5. H. E. Edgerton. Shockwave photography of large subjects in daylight. *Rev. Sci. Instruments,* Vol. 29(2), pp. 171-172, 1958.

6. J. K. Biele. Point-source spark shadowgraphy at the historic birthplace of supersonic transportation - A historical note. *Shock Waves* 13 (3):167-177, 2003.

7. S. P. Parthasarathy, Y. I. Cho, and L. H. Back. Wide-field shadowgraphy of tip vortices from a helicopter rotor. *AIAA J.* Vol. 25(1), pp. 64-70, 1987.

8. T. R. Norman and J. S. Light. Rotor tip vortex geometry measurements using the wide-field shadowgraph technique. *J. Amer. Helicopter Soc.* Vol. 32(2), pp. 40-50, 1987.

9. A. Bagai and J. G. Leishman. Improved wide-field shadowgraph set-up for rotor wake visualization. *J. Amer. Helicopter Soc.* Vol. 37(3) pp. 86-92, 1992.

10. 3M Industrial Adhesives and Tapes Division, Building 21-1W-10, 900 Bush Avenue, St. Paul, MN 55144-1000, fax 651-778-4244.

11. S. Winburn, A. Baker, and J. G. Leishman. Angular response properties of retroreflective screen materials used in wide-field shadowgraphy. *Exp. Fluids* Vol. 20(3), pp. 227-229, 1996.

12. Virtual Backgrounds, Inc., 101 Uhland Rd. Suite 108, San Marcos, TX 78666, (512)805-4844, fax(512)754-0316, info@virtualbackgrounds.net.

13. Tech Imaging Services, Inc., 27 Congress Street, Suite 501, Salem, MA 01970, Phone: 978-740-0063, Fax: 978-740-2769, jill@techimaging.com.

14. M. Philbert, J. Surget, and C. Veret. Shadowgraph and schlieren. In: Handbook of Flow Visualization, ed. W-J. Yang, Hemisphere Publishing Corp., Washington, pp. 189-217, 1989.

15. Stock number Y45-944, Edmund Industrial Optics, 101 E. Gloucester Pike, Barrington, NJ 08007-1380, (800) 363-1992, www.edmundoptics.com.

16. H. Kleine, J. M. Dewey, K. Ohashi, T. Mizukaki, and K. Takayama. Studies of the TNT equivalence of silver azide charges. *Shock Waves,* Vol. 13(2), pp. 123-138, 2003.

17. P. D. Smith, G. C. Mays, T. A. Rose, K. G. Teo, and B. J. Roberts. Small-scale models of complex-geometry for blast overpressure assessment. *Intl. J. Impact Eng.* Vol. 12(3), pp. 345-60, 1992.

18. E. M. Freemesser. Silencers: Testing and Protocols. In press, 2005.

19. H. Schardin. Die Schlierenverfahren und ihre Anwendungen. *Ergebnisse der Exakten Naturwissenschaften*, Vol. 20, pp. 303-439, 1942.

20. R. Varosh. Electric detonators: EBW and EFI. *Propellants Explosives Pyrotechnics* Vol. 21(3):150-154, 1996.